Large eddy simulation of turbulent flow of pseudoplastic and dilatant fluids: turbulence characteristics

Mohamed Abdi, Meryem Ould-Rouiss, Fatima Zohra Nedjda Bouhenni, Abdelfettah Menouer

Large Eddy Simulation of Turbulent Flow of Pseudoplastic and Dilatant Fluids: Turbulence Characteristics

Mohamed ABDI [a*], Meryem OULD-ROUISS [b], Fatima Zohra Nedjda BOUHENNI [c] Abdelfettah MENOUER [a]

(a) Laboratoire de génie électrique et des plasmas (LGEP) University of Tiaret, Algeria
(b) Laboratoire de Modélisation et Simulation Multi Echelle, MSME, Université Gustave Eiffel, UMR 8208 CNRS, 5 bd Descartes, 77454 Marne-la-Vallée, Paris, France
(c) Department of Mechanical Engineering, University Ibn Khaldoun, Tiaret 14000, Algeria
**E-mail: abdi.mohamed1@live.fr*

ABSTRACT

The current inquiry analysed the turbulent flow pattern of power-law fluids to shed light on the critical turbulence characteristics of non-Newtonian fluids. The flow behaviour index of the power-law fluid in the current investigation was set at 0.75, 0.8, 1, 1.2, 1.4, and 1.6 at a simulation's Reynolds number of 12000. This investigation was focused on large eddy simulation (LES) of turbulent pipe flow of pseudoplastic and dilatant fluids passing through an axially stationary pipe. The results point to a significant increase in the generation of axial turbulence and a noticeable decrease in the transfer of tangential and radial turbulence intensities from the axial intensities with a drop in the flow behaviour index. A substantial reduction of the turbulent kinetic energy and the Reynolds shear stress of velocity variations in the radial direction was another effect of the lower flow behaviour index.

KEYWORDS: Large eddy simulation (LES); Shear-thinning; Shear-thickening; Fully developed; Turbulent flow.

1. INTRODUCTION

Many fluids with potential for industrial applications exhibit non-Newtonian fluid behaviours, including polymer, petroleum, plastics, cement, food products, paper, and paint. Fully developed turbulent flow through a smooth pipe is a canonical problem in fluid mechanics and is significant in engineering. According to a literature review, several studies have been done on the turbulent flow of non-Newtonian fluid in recent years, including theoretical and experimental work [1-6] and numerical work [7-16].

Rudman et al. [10] applied direct numerical simulation (DNS) to simulate a fully developed turbulent flow of shear-thinning at various generalised Reynolds numbers for distinct flow behaviour indices (0.5, 0.69 and 0.75). DNS research was conducted by Gavrilova and Rudyak [14] at two generalised Reynolds values, 10000 and 20000, throughout a 0.4–1 power-law index range. Gavrilova and Rudyak [13] presented distributions of Reynolds stress tensor components, averaged viscosity, viscosity fluctuations, and measures of turbulent anisotropy with an emphasis on turbulent mean variables. By providing the distributions of the turbulent stress tensor components, the shear stress and turbulent kinetic energy balances, Gavrilova and Rudyak [14] published the same findings one year later with a focus on the energy balance and the shear stresses.

More recently, Abdi et al. [17] have conducted a fully developed turbulent forced convection of thermally independent pseudoplastic fluid with a flow behaviour index of 0.75 through an axially heated rotating pipe, by means of LES with an extended Smagorinsky model. With a rotation rate ranging from 0 to 3, where the simulation Reynolds and Prandtl numbers of the working fluid were assumed to be 4000 and 1, respectively. It is observed that as the pipe wall rotates, it is seen that the temperature along its radius noticeably decreases as the rotation rate increases. This is because the apparent fluid viscosity in the pipe's core region decreases, which causes a centrifugal force that causes the mean axial velocity profile to noticeably increase.

The present paper aimed to examine the effect of the power-law fluid's flow behaviour index (n) on turbulence statistics and instantaneous turbulence structure. Toward this end, a large eddy simulation (LES) with a standard dynamic model was devoted to a fully developed turbulent flow of shear-thinning (n<1) and shear-thickening (n>1) fluids across an isothermal stationary pipe. This study was performed at a simulation's Reynolds number of 12000, and the flow behaviour indexes were chosen to be 0.75, 0.8, 1, 1.2, 1.4 and 1.6.

2. GOVERNING EQUATIONS AND NUMERICAL PROCEDURE

2.1. Governing Equations

The study dealt numerically with a fully developed turbulent flow of power-law fluids in a pipe at different flow behaviour indexes ($0.75 \leq n \leq 1.6$) at a simulation Reynolds number of 12000, using the LES approach with a standard dynamic model with computational domain length of $20R$ (Fig.1). The filtered equations were expressed as follows (Equations 1 and 2):

$$\frac{\partial \overline{u}_i}{\partial x_i} = 0 \tag{1}$$

$$\frac{\partial \overline{u}_j}{\partial t} + \frac{\partial \overline{u}_i \overline{u}_j}{\partial x_i} = -\frac{d\overline{P}}{\partial x_j} + \frac{1}{\mathrm{Re}_s}\frac{\partial}{\partial x_i}\left[\overline{\dot{\gamma}^{n-1}}\left(\frac{\partial \overline{u}_j}{\partial x_i} + \frac{\partial \overline{u}_i}{\partial x_j}\right)\right] + \frac{\partial \overline{\tau}_{ij}}{\partial x_i} \tag{2}$$

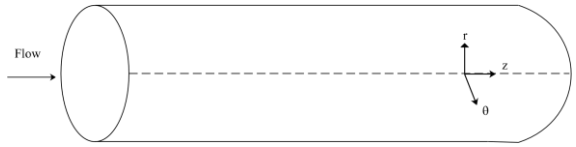

Figure 1: computational domain

2.2. Numerical Procedure

The mathematical model was implemented in a finite difference laboratory code. The governing equations were discretised on a staggered mesh in cylindrical coordinates with a computational length in the axial direction $20R$. The numerical integration was performed using a finite difference scheme, second-order accurate in space and time. The time advancement employed a fractional-step method. A third-order Runge-Kutta explicit scheme and a Crank-Nicholson implicit scheme were used to evaluate the convective and diffusive terms, respectively. In the non-Newtonian Smagorinsky model, the subgrid stress tensor $\overline{\tau}_{ij}$ is linked to the strain rate tensor by $\overline{\tau}_{ij} = -2\nu_t \overline{S}_{ij}$.

3. RESULTS AND DISCUSSION

The goal was to reveal the influence of the flow behaviour index of the pseudoplastic (shear-thinning) and dilatant (shear-thickening) fluids on the turbulent flow statistics and instantaneous turbulence structure along the radial direction, especially in the vicinity of the wall. Fig.3 compares the turbulence intensities of the Newtonian fluid with that of Redjem et al. [18] at the Reynolds number of 5500; the results present the root mean square (RMS) distribution of the axial, radial and tangential velocity fluctuations of the Newtonian fluid (n=1). As shown in Fig.3, the RMS of the axial components were in excellent agreement along the pipe radius with that of the literature; the tangential and radial components were also in accord with the results of Redjem et al. [18]. There was little discrepancy due to the difference in the Reynolds number value and the numerical solution procedure.

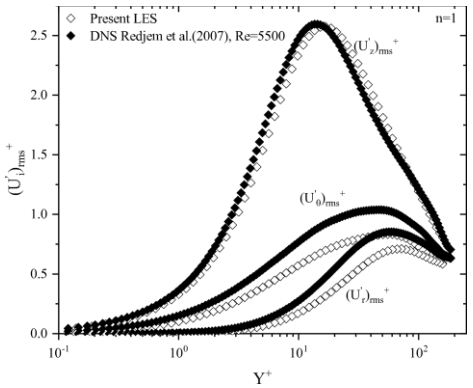

Figure 2: Validation

3.1. Root mean squares of velocity fluctuations

The root mean square (RMS) distribution of the axial, tangential and radial velocity fluctuations of the pseudoplastic and dilatant fluids along the pipe radius (R) are presented in Figures 3-5, respectively. These profiles were scaled by the friction velocity versus the distance from the wall in wall units Y^+. The flow behaviour indexes were set at 0.75, 0.8 (shear-thinning), 1.2, 1.4, 1.6 (shear-thickening) and 1 (Newtonian) at a simulation Reynolds number of 12000.

Based on the DNS data of Redjem et al. [18], the accuracy and reliability of the predictions and numerical method have been confirmed decisively. As shown in Fig.2, the current RMS is in excellent agreement with the results of Redjem et al. [18], where no significant differences were found between them.

As shown in Fig.3, the power-law and Newtonian fluids exhibited a similar trend along the pipe radius, where there was a clear trend of increase in these profiles over the radial direction. The RMS of the axial components was almost identical for all fluid behaviour indices in the vicinity of the wall up to approximately (Y^+= 10), where it could be said that the RMS of the axial component was almost independent of the flow behaviour index in this region. These profiles began to deviate from each other further away from the wall towards the core region; this deviation became more distinct with distance from the wall (Y^+), especially in the logarithmic region ($30\leq Y^+\leq 200$). As seen in Fig.3, the RMS of the axial component enhanced or increased gradually away from the wall with the wall distance up to approximately (Y^+= 10) because of axial fluctuation generation in the near-wall region, as pointed out by Gavrilov and Rudyak [13]. At a large wall distance, the axial profiles began to drop rapidly to lower values in the core region for all fluid behaviour indices; this meant that the axial fluctuations vanished gradually in this flow region.

It was evident that the decreased flow behaviour index resulted in a pronounced enhancement in the RMS of the axial velocity fluctuations beyond the buffer region ($5\leq Y^+\leq 30$). Moreover, this reduction in the flow index led also to a shift in the peak location slightly away from the wall toward the core region. The axial velocity fluctuations were generated in the wall's vicinity and transported from the near-wall region toward the core region, as pointed out by previous researchers [13]. It can be said that with a decreasing flow behaviour index, the generation of the axial velocity fluctuations enhanced considerably, where this decrease in the flow index also led to ameliorating or improving the transport of the axial velocity fluctuations from the wall vicinity towards the core region.

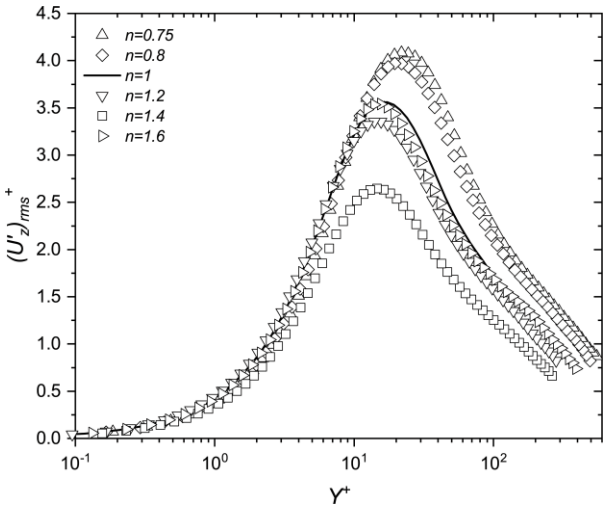

Figure 3: RMS of axial component

As shown in Fig.4, the same trend of RMS of tangential fluctuations was observed along the pipe radius for all flow behaviour indices; the tangential fluctuations were almost negligible in the near-wall region, where this was ascribed to the molecular shear stress being the dominant force compared to the turbulent one in this region. These profiles began to increase gradually and deviated from each other away from the near-wall region with distance from the wall (Y^+). They dropped rapidly and fell to lower values beyond approximately (Y^+= 30) for all flow behaviour indices. As seen in Fig.4, the RMS of tangential fluctuations of the dilatant fluids lay above the pseudoplastic along the pipe radius, as the flow behaviour index was decreased as the RMS of tangential fluctuations was attenuated or diminished along the pipe radius. The peak locations were shifted towards the core region. It was evident that the decreased flow index induced a

noticeable reduction in the transfer of the tangential fluctuations from the axial ones, consequently in the tangential fluctuations. This decreased flow behaviour index also ameliorated the transport of the tangential fluctuations from the wall vicinity towards the core region. It was worth noting that these predicted results were in line with those of Gavrilov and Rudyak [13].

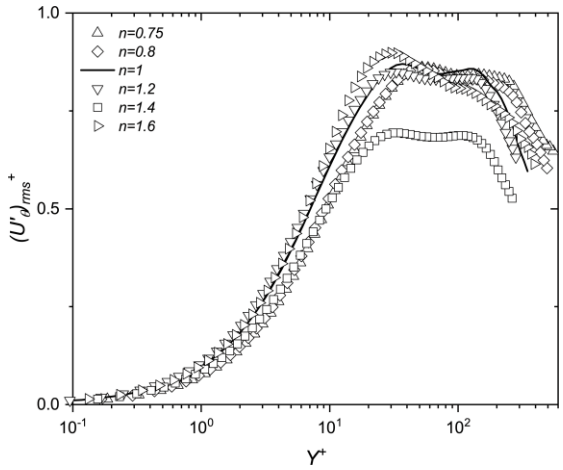

Figure 4: RMS of the tangential component

As seen in Fig.5, the RMS of radial fluctuations was identical for all flow behaviour indices and equal to zero in the viscous sublayer ($5 \leq Y^+ \leq 30$) up to approximately ($Y^+ = 3$). Beyond $Y^+ = 3$, these profiles exhibited a significant enhancement further away from the wall towards the core region. Beyond ($Y^+ = 50$), these profiles fell off rapidly to lower values after reaching their maximum values. It should be noted that with a reducing flow behaviour index (n), the radial fluctuations reduced significantly along the pipe radius, and the predicted peak locations shifted away towards the core region, as Gavrilov and Rudyak [13]. It can be said that the decreasing flow behaviour index yielded an attenuation in the radial fluctuation, which meant reducing the fluctuations transfer from the axial to the radial one and ameliorating the transport of the radial fluctuations from the near-wall towards the core region.

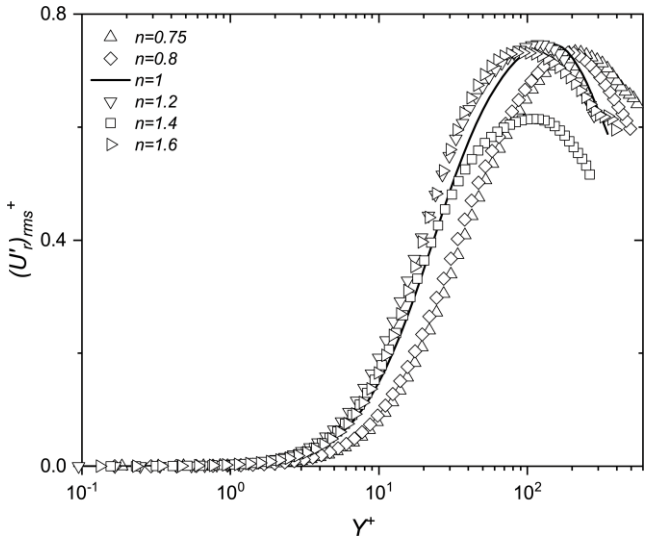

Figure 5: RMS of the radial component

3.2. Turbulent Kinetic energy

The turbulent kinetic energy of the pseudoplastic and dilatant fluids along the pipe radius (R) versus the distance from the wall in wall units Y^+ are depicted in Fig.6, at a flow behaviour index of ($0.75 \leq n \leq 1.6$) and at a simulation Reynolds number of 12000. Overall, the kinetic energy of turbulent fluctuations exhibited almost the same trend as the axial turbulence intensities, which were almost independent of the flow behaviour index and equal to zero in the near-wall region: molecular shear stress was the dominant force in this region. It was important to note that the observed increased and decreased turbulent kinetic energy with

the wall distance were related to the enhancement and reduction, respectively, of the axial turbulence intensities over the pipe radius, the increased turbulent kinetic energy beyond the buffer region was raised because the generation of the axial turbulence intensities and transfer of these fluctuations to the tangential and radial ones, as pointed out by other studies [13]. It was worth noting that the turbulent kinetic energy attenuated pronouncedly over the radial direction with a decreasing flow behaviour index.

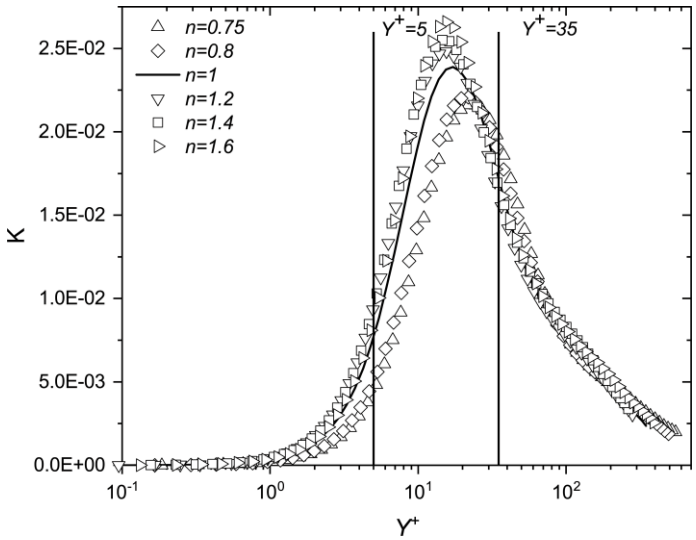

Figure 6: Turbulent kinetic energy

3.3. Turbulent Reynolds shear stress

The turbulent Reynolds shear stress of the axial and radial velocity fluctuations of the shear-thinning, shear-thickening and Newtonian fluids were also assessed. In the viscous sublayer, the Reynolds shear stress profiles were identical and equal to zero. This was due to the absence of velocity fluctuations near the wall region. Out of the viscous sublayer, the Reynolds stress profiles deviated from each other and increased sharply to reach their peak value in the buffer region, as shown in Fig.7. This enhancement was related to the generation of the axial fluctuations further away from the wall (Fig.3). Moreover, these profiles fell off rapidly to a zero value in the core region. This was attributed to a vanishing of the axial and radial velocity fluctuation in this region (Fig.3 and Fig.4). It was worth noting that when the flow behaviour index decreased, the Reynolds shear stress of the axial, radial velocity fluctuations reduced considerably along the pipe radius (Fig.7).

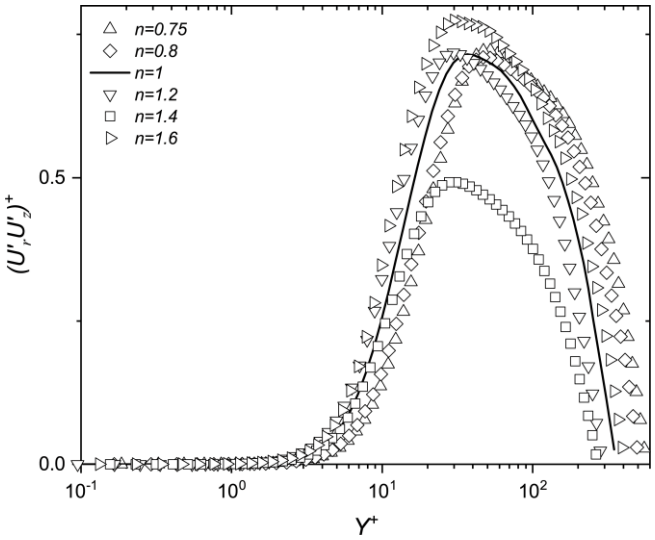

Figure 7: Turbulent Reynolds stress

3.4. Higher-order statistics

Fig.8 and Fig.9 display respectively the skewness and flatness of the axial velocity fluctuations distribution against the distance from the wall in wall units Y^+ at R_{es}=12000 for $0.4 \leq n \leq 1.6$. The skewness

and flatness were almost identical for all flow behaviour indices along the pipe radius. These profiles exhibited a rapid drop in the vicinity of the wall. The skewness tended to the Gaussian value ($S(U'_z) = 0$), while the flatness also tended to the Gaussian value ($F(U'_z) = 3$) for all flow behaviour indices. It can be said here that the skewness and flatness of the pseudoplastic and dilatant fluids were almost independent of the flow behaviour index along the pipe radius.

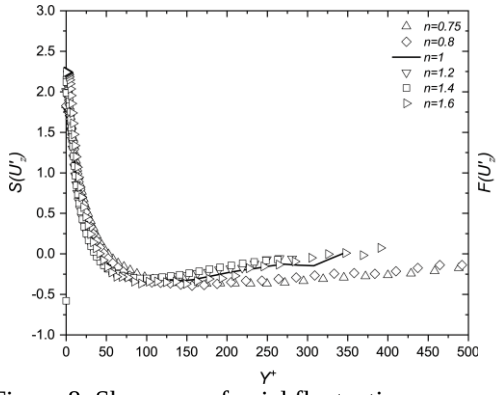

Figure 8: Skewness of axial fluctuations

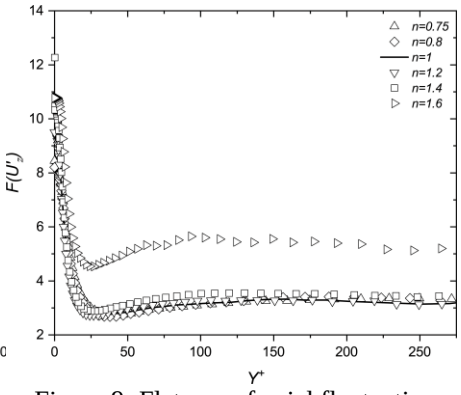

Figure 9: Flatness of axial fluctuations

4. CONCLUSIONS

Using a large eddy simulation (LES) and a universal dynamic model, a fully developed turbulent flow of pseudoplastic and dilatant fluids through an isothermal stationary pipe was examined numerically. This investigation was conducted using a simulation with a Reynolds number of 12000 and a flow behaviour index of $0.75<n<1.6$. The results indicated that the flow behaviour index dropped, which caused an increase in the generation of axial turbulence and a noticeable decrease in the transfer of tangential and radial turbulence intensities from the axial intensities. Additionally, this drop in the flow behaviour index improved the conveyance of the axial, radial and tangential turbulence intensities from the wall proximity to the core region. The turbulent kinetic energy and Reynolds shear stress of velocity variations decreased significantly in the radial direction with a decreasing flow behaviour index. On the other hand, the pseudoplastic and dilatant fluids' skewness and flatness seem nearly independent of the flow behaviour index.

NOMENCLATURE

U_b	Average velocity, $\left(m.s^{-1}\right)$
U_τ	Friction velocity $U_\tau = \left(\tau_w/\rho\right)^{1/2}$, $\left(m.s^{-1}\right)$
U_{CL}	Centreline axial velocity for analytical fully developed laminar profile $U_{CL} = \left(3n+1\right)U_b/\left(n+1\right)$, $\left(m.s^{-1}\right)$
R	Pipe radius, $\left(m\right)$
n	Flow index
K	Consistency index $\left(pa.s^n\right)$
Y^+	Wall distance $Y^+ = \rho U_\tau Y/\eta_w$
f	Friction factor $f = 2\tau_W/\left(\rho U_b{}^2\right)$
Re_s	Reynolds number of the simulations $\mathrm{Re}_s = \rho U_{CL}{}^{2-n}R^n/K$
Greek symbols	
$\dot{\gamma}$	Shear rate $\dot{\gamma} = \sqrt{S_{ij}S_{ij}}$
η	apparent viscosity $\eta = K\dot{\gamma}^{n-1}$
ρ	Density

$\overline{\tau}_{ij}$	Subgrid stress tensor $\overline{\tau}_{ij} = -2\nu_t \overline{S}_{ij}$
Subscripts	
z, r, θ	Axial, radial, tangential velocity
C	Centreline
L	Laminar
s	Simulation
w	Wall
Superscripts	
$\langle\ \rangle$	Statistically averaged
$(\ )^+$	Normalised by U_τ

Figure	Captions
Figure 1	computational domain
Figure 2	Validation.
Figure 3	Figure 3: RMS of axial component.
Figure 4	RMS of the tangential component.
Figure 5	RMS of the radial component.
Figure 6	Turbulent kinetic energy.
Figure 7	Turbulent Reynolds stress
Figure 8	Skewness of axial fluctuations
Figure 9	Flatness of axial fluctuations

Figures list.

REFERENCES

[1]. A. B. Metzner, and J. C. Reed: Flow of non-Newtonian fluids-correlation of the laminar, transition, and turbulent-flow regions. J. AIChE. vol 1, no. 4 (Dec. 1955) 434-440.

[2]. A. B. Metzner: Non-Newtonian Fluid Flow. Relationships between Recent Pressure-Drop Correlations. Ind. Eng. Chem. vol. 49, no. 9 (Sep 1957) 1429-1432.

[3]. D. W. Dodge and A. B. Metzner: Turbulent flow of non-newtonian systems. AIChE J. vol. 5, no. 2 (Jun. 1959) 189-204.

[4]. Y. TOMITA: A Study on Non-Newtonian Flow in Pipe Lines. Bull. JSME, vol. 2, no. 5. (1959) pp. 10–16.

[5]. V. Vidyanidhi and A. Sithapathi: Non-Newtonian Flow in a Rotating Straight Pipe. J. Phys. Soc. Japan, vol. 29, no. 1. (Jul. 1970) pp. 215–219.

[6]. F. T. Pinho and J. H. Whitelaw: Flow of non-newtonian fluids in a pipe. J. Nonnewton. Fluid Mech., vol. 34, no. 2. (Jan. 1990) pp. 129-144.

[7]. M. R. Malin: Turbulent pipe flow of power-law fluids. Int. Commun. Heat Mass Transf., vol. 24, no. 7. (Nov. 1997) pp. 977-988.

[8]. M. Malin: The Turbulent Flow of Bingham Plastic Fluids in Smooth Circular Tubes. Int. Commun. Heat Mass Transf., vol. 24, no. 6. (Oct. 1997) pp. 793-804

[9]. M. Malin: Turbulent pipe flow of Herschel-Bulkley fluids. Int. Commun. Heat Mass Transf., vol. 25, no. 3. (Apr. 1998) pp. 321-330.

[10]. M. Rudman, H. M. Blackburn, L. J. W Graham, and L. Pullum: Turbulent pipe flow of shear-thinning fluids. J. Nonnewton. Fluid Mech., vol. 118, no. 1. (Mar. 2004) pp. 33-48.

[11]. T. Ohta and M. Miyashita: DNS and LES with an extended Smagorinsky model for wall turbulence in non-Newtonian viscous fluids. J. Nonnewton. Fluid Mech., vol. 206. (Apr. 2014) pp. 29-39.
[12]. P. S. Gnambode, P. Orlandi, M. Ould-Rouiss, and X. Nicolas: Large-Eddy simulation of turbulent pipe flow of power-law fluids. Int. J. Heat Fluid Flow. vol. 54 Aug. 2015 pp. 196-210
[13]. A. A. Gavrilov and V. Y. Rudyak: Direct numerical simulation of the turbulent flows of power-law fluids in a circular pipe. Thermophys. Aeromechanics, vol. 23, no. 4 (Jul. 2016) pp. 473-486.
[14]. A. A. Gavrilov and V. Y. Rudyak: Direct numerical simulation of the turbulent energy balance and the shear stresses in power-law fluid flows in pipes. Fluid Dyn., vol. 52, no. 3 (May 2017) pp. 363-374.
[15]. J. Singh, M. Rudman, and H. M. Blackburn: The influence of shear-dependent rheology on turbulent pipe flow. J. Fluid Mech., vol. 822. (Jul. 2017) pp. 848-879.
[16]. J. Singh, M. Rudman, and H. M. Blackburn: The effect of yield stress on pipe flow turbulence for generalised newtonian fluids. J. Nonnewton. Fluid Mech., vol. 249, (Nov. 2017) pp. 53-62.
[18] M. Abdi, A. Noureddine, and M. Ould-Rouiss, "Numerical simulation of turbulent forced convection of a power law fluid flow in an axially rotating pipe," J. Brazilian Soc. Mech. Sci. Eng., vol. 42, no. 1, p. 17, 2020.
[18]. L. Redjem-Saad, M. Ould-Rouiss, and G. Lauriat: Direct numerical simulation of turbulent heat transfer in pipe flows: Effect of Prandtl number. Int. J. Heat Fluid Flow, vol. 28, no. 5. (Oct. 2007) pp. 847–861.